# Monte Carlo Methods Final Project

Jacopo Omodei

September 10, 2025

## 1 Introduction and background

In high-energy physics, the process of electron–positron annihilation serves as a clean and well-controlled environment to study the production of resonant states. When an electron and a positron collide at a center-of-mass (CM) energy close to the mass of a bound state, such as the charmonium resonances $J/\psi$ and $\psi(2S)$, the total cross section exhibits a sharp enhancement known as a resonance peak. The shape of these peaks encodes essential information about the dynamics of quantum electrodynamics (QED) and the properties of the resonances themselves. The study of these resonance peaks has been crucial to the advancement of the standard model as we know it today. This simulation will aim to recreate the results outlined in the Nobel lecture [1] and will therefore use the same experimental parameters as the *SPEAR* electron positron storage ring and the *MK1* magnetic detector outlined in the paper.

The resonance structure is well described by the **Breit–Wigner** formula, which models the cross section for producing a resonance of mass $M$ and total width $\Gamma$ through $e^+e^-$ annihilation at a certain center of mass energy $s$.

$$\sigma_{BW}(s) = \frac{2J+1}{(2S_{e^-}+1)(2S_{e^+}+1)} \frac{4\pi}{s^2} \left[ \frac{\Gamma^2/4}{(\sqrt{s}-M)^2 + \Gamma^2/4} \right] B_{ee}^2 \qquad (1)$$

The first terms handle the spin degeneracy of the various particles and can be replaced with $S_{e^+} = S_{e^-} = \frac{1}{2}$ and $J = 1$, while $B_{ee}$ is the branching ration of the resonance decay into the $e^+e^-$ state and can be found alongside $\Gamma$ in the PDG [2]. This formalism accounts for the narrow enhancement in the cross section at $\sqrt{s} \approx M$.

For narrow vector mesons such as the $J/\psi$, the resonance signal is particularly pronounced against the smooth background, whose differential cross section follows, at the leading order, **Bhabha** scattering.

$$\frac{d\sigma_{bg}}{d\cos\theta} = \frac{\pi \cdot \alpha^2}{s}\left[\frac{s^2+u^2}{t^2} + \frac{t^2+u^2}{s^2} + \frac{2u^2}{s \cdot t}\right] \tag{2}$$

Where $\alpha$ represents the fine-structure constant and $s$, $t$, $u$ represent the Mandelstam variables of the process, which simplify to

$$\begin{aligned} t &= -\frac{s}{2}(1-\cos\theta) \\ u &= -\frac{s}{2}(1+\cos\theta) \end{aligned} \tag{3}$$

To obtain the total cross section this must be integrated over $\cos\theta$ within the detector's angular acceptance limits, which for the *MK1* detector corresponds to an angular cut of $|\cos\theta| < 0.6$.

These two effects sum to produce theoretical resonance curves for the process at the lowest order, but many other higher-order effects plague the experiment. One such effect is the possibility of an initial state lepton losing energy due to the emission of a photon, lowering the CM energy of the interaction. This effect is called **Initial state radiation** (ISR) and is responsible for a smear in the resonance shape by shifting events to lower energies. This is a universal QED effect and must be accounted for in precision comparisons between theory and experiment. At the lowest order, it can be modeled by decreasing the CM energy by a fraction $x$, drawing from the following probability density function, peaked at low energy losses [3]. The leading-order approximation for this effect is the following.

$$\begin{aligned} p(x) &= k \cdot \frac{1+(1-x)^2}{x} \\ s' &= (1-x) \cdot s \end{aligned} \tag{4}$$

Where $k$ is the normalization factor. In practice, the observed resonance line shape at the order in which I will be studying it is thus a convolution of the intrinsic Breit–Wigner form with detector resolution and ISR effects, superimposed on the smooth QED background.

# 2 Project Framework

The guiding principle is to replicate, as closely as possible, the experimental conditions under which the $J/\psi$ and $\psi(2S)$ resonances were originally studied, thereby reproducing the characteristic resonance peaks and their distortions due to higher-order effects.

The project is organized into three components:

1. **Simulation:** A Monte Carlo algorithm generates pseudo-data by sampling from the theoretical probability distributions, while applying experimental effects such as detector resolution and statistical fluctuations. This pseudo-data mimics what a real experiment would record.
2. **Theory curve calculation:** Theoretical cross section curves are generated from the Breit–Wigner resonance shape combined with the Bhabha scattering background. Initial state radiation (ISR) effects are incorporated to model the energy loss of the incoming leptons, leading to the characteristic smearing of the resonance peak. These theoretical curves are convoluted along with gaussian curves to factor in experimental factors.
3. **Comparison:** Simulation results are compared directly with the theoretical curves, allowing me to evaluate how well the simulated data reproduces the expected resonance structure under realistic experimental conditions.

In order to produce realistic pseudo-data, several experimental and physical considerations are taken into account, drawing inspiration from the real-life detectors that were historically used for this experiment:

- **Beam energy spread:** In a storage ring, the beam energy is not perfectly monochromatic. This spread causes an additional broadening of the observed resonance peaks and must be folded into the simulation.
- **Detector resolution:** The measurement of the final-state leptons introduces uncertainties in the CM energy, which are modeled as Gaussian smearing of the true values.
- **Angular acceptance:** The detector does not have full $4\pi$ coverage. For the *MK1* detector, events are restricted to $|\cos\theta| < 0.6$, limiting the available phase space and modifying the effective cross section.
- **Statistical fluctuations:** The number of events observed at each energy point follows Poisson counting statistics, reflecting the finite integrated luminosity of the experiment.
- **ISR effects:** As photons are radiated by the incoming leptons, the effective center-of-mass energy of the interaction is reduced, redistributing events from the peak region to lower energies

This framework ensures that the simulation does not simply reproduce the idealized Breit–Wigner peak, but also incorporates the experimental realities that shape the data.

### 2.1 Monte Carlo Simulation of Pseudo-Data

The simulation of pseudo-data proceeds by mimicking, as closely as possible, the sequence of effects that govern a real $e^+e^-$ scattering experiment. The central idea is to start from a chosen nominal center-of-mass (CM) energy and generate a statistical sample of events that incorporates the physical distortions and experimental limitations. The procedure can be summarized as follows:

1. **Nominal energy:** For each scan point, the experiment is assumed to run at a fixed nominal CM energy $E_{\text{nom}}$. This represents the target energy set in the accelerator.

2. **Initial State Radiation (ISR):** If enabled, each event is assigned an ISR energy-loss fraction $x$, sampled from the QED radiator function (4)

3. **Gaussian smearing:** To account for the finite beam energy spread and detector resolution, the effective CM energy is further smeared by sampling from a Gaussian distribution with standard deviation

$$\sigma_E = \sqrt{\sigma^2_{\text{beam}} + \sigma^2_{\text{detector}}}. \tag{5}$$

   In our case, both $\sigma_{beam}$ and $\sigma_{detector}$ are equal to $3MeV$, which is very small considering the resonance mass of $3.096GeV$. However, one must keep in mind the *width* of the resonance rather than the mass, which turns out to be around $92.9keV$. Factoring in our experimental resolution will have the effect of greatly broadening the expected B-W peak.

   At each nominal energy, $N_{mc}$ points are drawn from this Gaussian distribution and averaged to obtain one *observed* energy.

4. **Cross section evaluation:** At each observed energy, the cross section is computed as the sum of:

   - Resonant contributions, modeled by Breit–Wigner functions for the $J/\psi$ and $\psi(2S)$, multiplied by the detector angular acceptance factor.
   - The non-resonant Bhabha scattering background, evaluated at the nominal energy.

5. **Conversion to counts:** The integrated luminosity $L_{\text{int}}$ (instantaneous luminosity $L_{\text{inst}}$ times the time per measurement) is used to convert the expected cross section into an expected number of events:

$$N_{\text{expected}} = \sigma \times L_{\text{inst}} \times t.$$

6. **Poisson fluctuations:** To simulate statistical fluctuations in the counting experiment, the observed number of events is drawn from a Poisson distribution with mean $N_{\text{expected}}$.

7. **Extraction of measured cross section:** The pseudo-measured cross section is obtained by inverting the luminosity relation,

$$\sigma_{\text{meas}} = \frac{N_{\text{observed}}}{L_{\text{int}}},$$

with an associated statistical uncertainty

$$\Delta\sigma = \frac{\sqrt{N_{\text{observed}}}}{L_{\text{int}}}.$$

8. **Error assignment:** The vertical axis uncertainties on the pseudo-data are given by the Poisson error above, while the horizontal axis uncertainties reflect the Gaussian energy resolution scaled by the effective statistics,

$$\Delta E = \frac{\sigma_E}{\sqrt{N_{\text{MC}}}},$$

where $N_{\text{MC}}$ is the number of Monte Carlo trials per scan point.

This procedure ensures that each simulated point in the resonance scan reflects both the underlying physics (Breit–Wigner resonances, ISR, Bhabha background) and the experimental realities (beam spread, detector resolution, finite luminosity, Poisson statistics). The resulting pseudo-data can then be directly compared to theoretical curves to validate the implementation and study the interplay of different effects.

## 2.2 Theoretical Cross Section Curves

In order to compare the pseudo-data with analytic expectations, theoretical cross section curves must be computed that incorporate the same physical effects responsible for shaping the observed resonance lines. While the underlying resonance structure is described by the Breit–Wigner formula, additional effects such as initial state radiation (ISR) and detector smearing must be included to obtain realistic predictions. This is achieved through successive convolutions applied on a fine energy grid.

1. **Breit–Wigner resonances:** The base cross section is calculated as the sum of two Breit–Wigner distributions describing the $J/\psi$ and $\psi(2S)$ resonances multiplied by the detector angular acceptance factor (just like in the simulation). This represents the idealized resonance structure in the absence of background or smearing.

2. **Addition of background:** The resonant signal is supplemented by the Bhabha scattering contribution,

$$\sigma_{\text{tot}}(s) = \sigma_{\text{res}}(s) + \sigma_{\text{Bhabha}}(s),$$

where the background is integrated over the experimental angular acceptance.

3. **Convolution with ISR radiator:** To account for QED initial state radiation, the cross section is convoluted with the ISR probability density function $p(x)$:

$$\sigma_{\text{ISR}}(s) = \int_0^1 p(x)\, \sigma_{\text{tot}}\big((1-x)\, s\big)\, dx.$$

This step redistributes events toward lower effective energies, smearing and distorting the resonance shape in a universal way independent of the detector.

4. **Gaussian smearing:** To model the finite beam energy spread and detector resolution, the ISR-modified cross section is further convolved with a Gaussian kernel of width (5). The convolution,

$$\sigma_{\text{smeared}}(E) = \int_{-\infty}^{\infty} \sigma_{\text{ISR}}(E') \cdot \frac{1}{\sqrt{2\pi}\, \sigma_E} \exp\left[-\frac{(E-E')^2}{2\sigma_E^2}\right] dE',$$

produces the final theory curve that directly reflects the expected outcome of a real detector.

5. **Fine energy grid:** Since these convolutions are carried out numerically, the calculation is performed on a dense energy grid. This ensures that the sharp resonance peaks and narrow structures introduced by ISR are correctly resolved.

The resulting theoretical curves represent the best-possible prediction of the experiment in the absence of statistical fluctuations. They can therefore be used as a baseline for validating the Monte Carlo simulation.

# 3 Results and Conclusions

## 3.1 Results

The comparison between the pseudo-data obtained from the Monte Carlo simulation and the theoretical curves is shown in Figures 1 and 2.

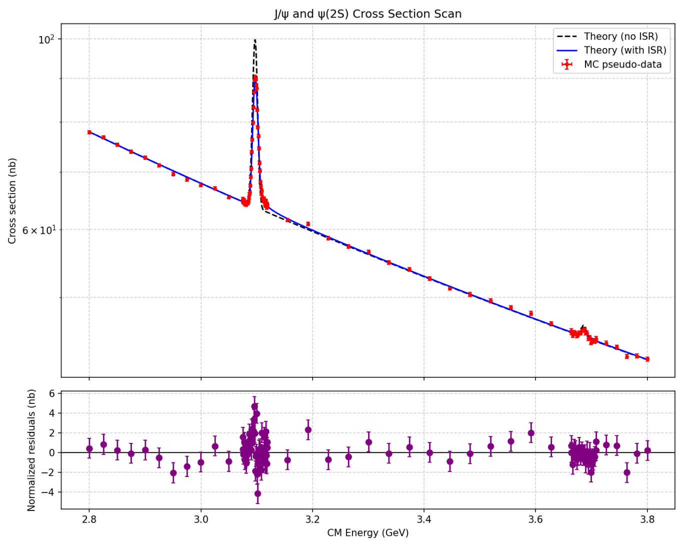


Figure 1: Comparison of Monte Carlo pseudo-data with the theoretical prediction for the full energy scan. Error bars on the pseudo-data reflect Poisson count fluctuations (vertical) and Gaussian beam smearing (horizontal). Normalized residuals are shown

Overall, the Monte Carlo results reproduce the expected resonance structures and backgrounds, validating the simulation framework. However, slight mismatches between theory and pseudo-data can be observed, particularly in proximity of the peaks. These differences can be attributed to several factors:

- **Statistical limitations:** The number of Monte Carlo samples ($N_{\mathrm{MC}}$) directly impacts the precision of the pseudo-data. Increasing $N_{\mathrm{MC}}$ reduces fluctuations and improves agreement.
- **Numerical approximations:** Both the ISR convolution and the Gaussian smearing are computed numerically. Approximations in the integration (e.g. discretization, finite grid spacing) can lead to small but systematic deviations.

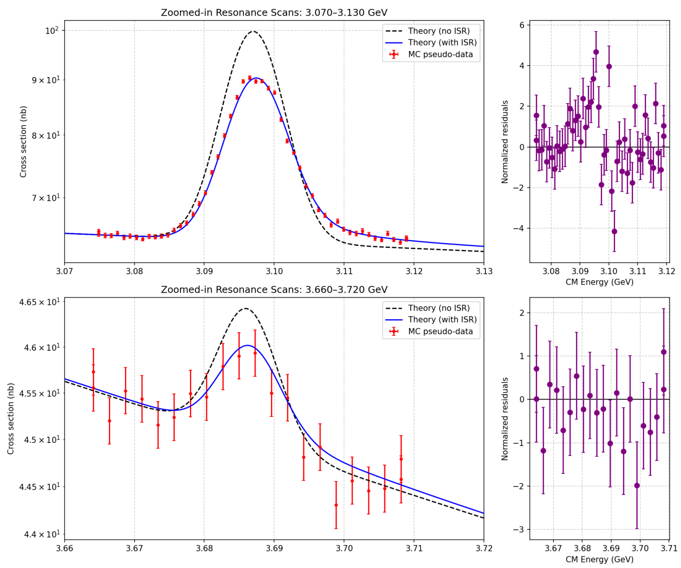


Figure 2: Comparison of Monte Carlo pseudo-data with the theoretical prediction around the two resonances, for clarity.

These effects, which are generally reduced by increasing the number of Monte Carlo samples and thinning the grid spacing for the numerical convolutions, are especially prominent given the resonant nature of the problem.

## 3.2 Conclusions and Outlook

This project successfully demonstrates how a Monte Carlo simulation can reproduce the effects of initial state radiation, detector smearing, and statistical fluctuations in the study of narrow resonances such as the $J/\psi$ and $\psi(2S)$. The comparison with convolved theoretical curves highlights the importance of including experimental effects in precision measurements.

Several natural extensions could be explored:

- **Alternative channels:** Repeating the study with $\mu^+\mu^-$ or hadronic final states, potentially summing them to obtain the complete resonance form.
- **Additional radiative effects:** Including bremsstrahlung radiation or final state radiation (FSR), which further modify the observed cross sec-

tion.

- **Efficiency improvements:** Precomputing the ISR–Gaussian convolution on a fine grid and storing it in a lookup table, speeding up the time it takes to evaluate the theoretical curve (by using, for example, linear interpretation or a spline).

In summary, this project highlights how Monte Carlo methods compliment theoretical models, and their utility in high energy physics research.

## References


[1] Burton Richter, "From the psi to charm - the experiments of 1975 and 1976," Dec 1976.

[2] S. Navas et al., "Review of particle physics," *Phys. Rev. D*, vol. 110, no. 3, pp. 030001, 2024.

[3] V. P. Druzhinin, S. I. Eidelman, S. I. Serednyakov, and E. P. Solodov, "Hadron production via," *Reviews of Modern Physics*, vol. 83, no. 4, pp. 1545–1588, Dec 2011.